Supplementary information to

Centennial-scale intensifications of the Atlantic Meridional Overturning Circulation during Heinrich Stadial 1

Partha Sarathi Jena, Cristiano Mazur Chiessi, Ines Beese, Martin Butzin, Bruna Borba Dias, Marília de Carvalho Campos, Gerrit Lohmann, Stefan Mulitza

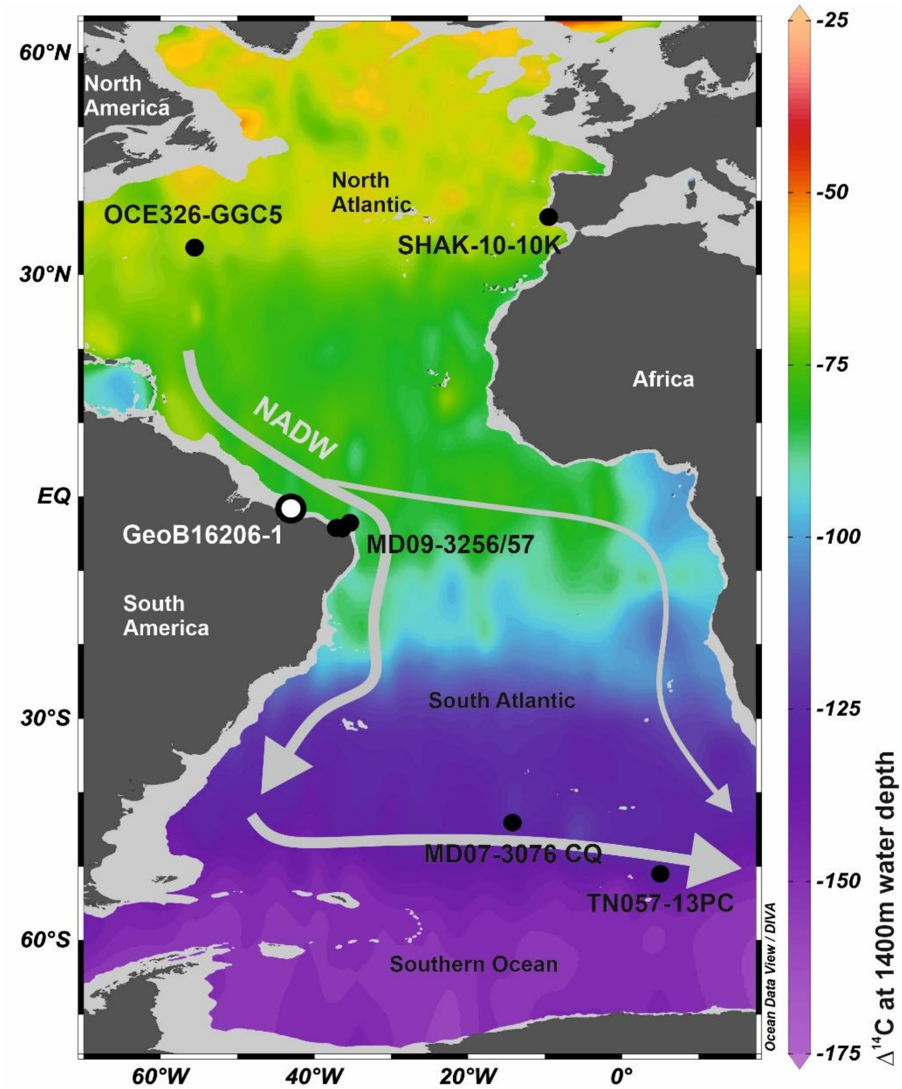

Supplementary Fig. 1: Location of marine sediment core GeoB16206-1 (white circle) collected from the western equatorial Atlantic Ocean. In the background, the radiocarbon concentration of dissolved inorganic carbon ($\Delta^{14}C$)[1] at 1400 m water depth (representing the bottom of the water column at the site of core GeoB16206-1) is shown. The grey arrows schematically represent northern-sourced water flow in the Atlantic mid-depths[2]. The $\Delta^{14}C$ values show an ageing trend of mid-depth northern-sourced waters (i.e., North Atlantic Deep Water (NADW)) from the North Atlantic towards the South Atlantic. The solid black circles indicate selected sites discussed in the text[3–6]. The figure was partially prepared using Ocean Data View[7].

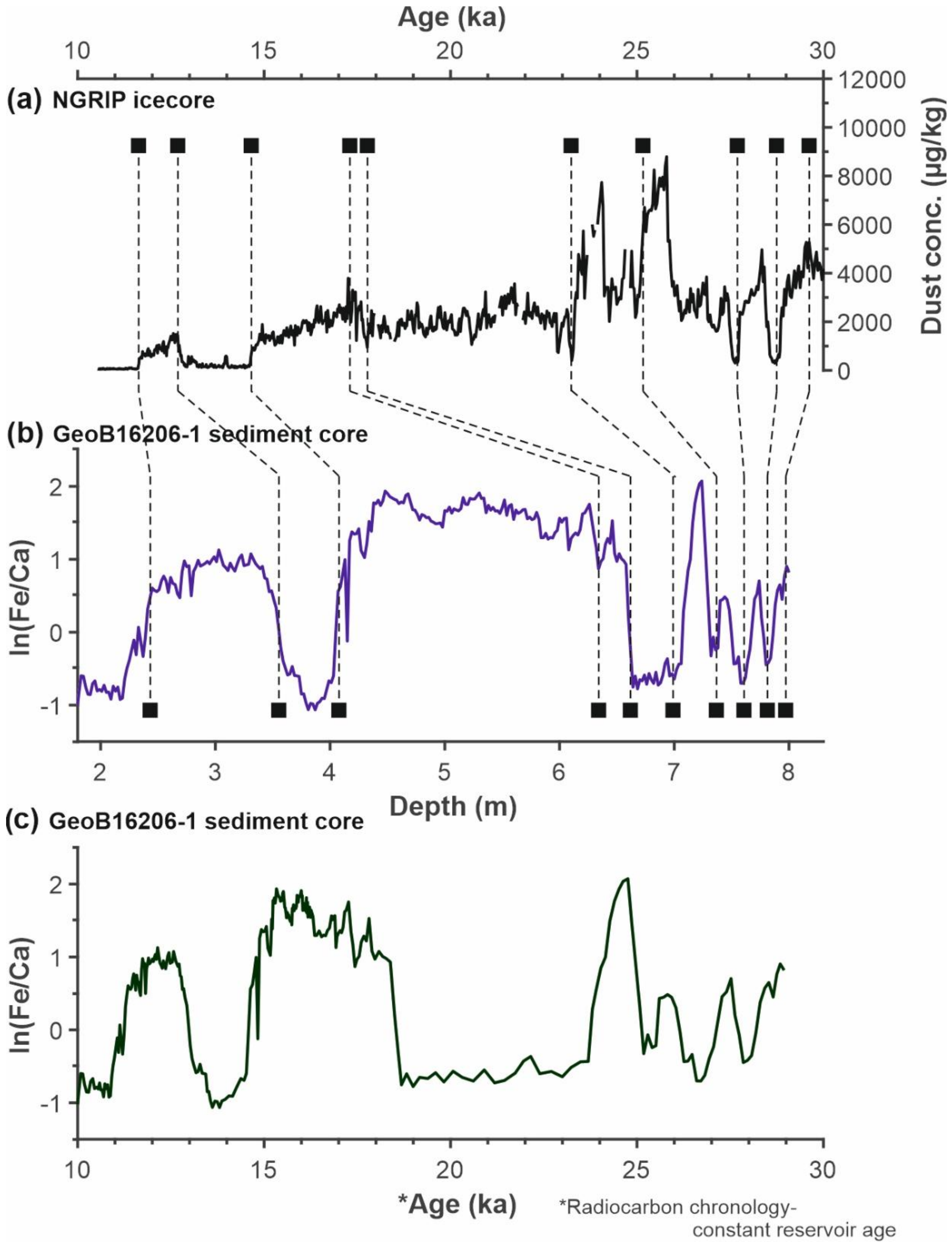

Supplementary Fig. 2: The chronology of the marine sediment core GeoB16206-1 derived from stratigraphic peak matching. (a) High-resolution NGRIP dust record[8] on the GICC05 time scale[9] (b) ln(Fe/Ca) record from sediment core GeoB16206-1[10]. The ln(Fe/Ca) record, on the chronology derived by using the planktic foraminifera radiocarbon ages[11] with a constant reservoir age is also shown in (c) for comparison.

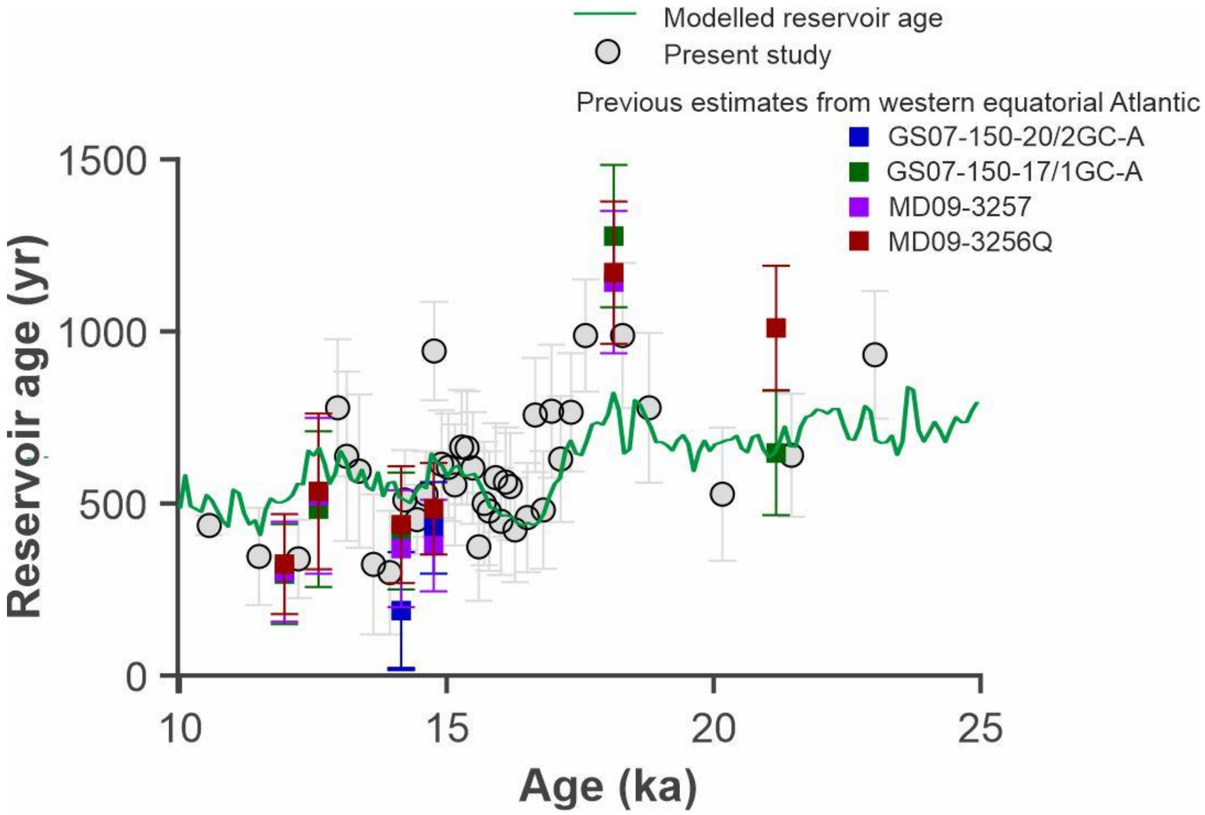

Supplementary Fig. 3: Surface reservoir age estimates (grey circles) for marine sediment core GeoB16206-1. The reservoir age estimates from the present study are compared with previous estimates for the intermediate and deep western equatorial Atlantic Ocean (coloured squares)[3] and model simulations (CLIMBER-X[12]; green curve).

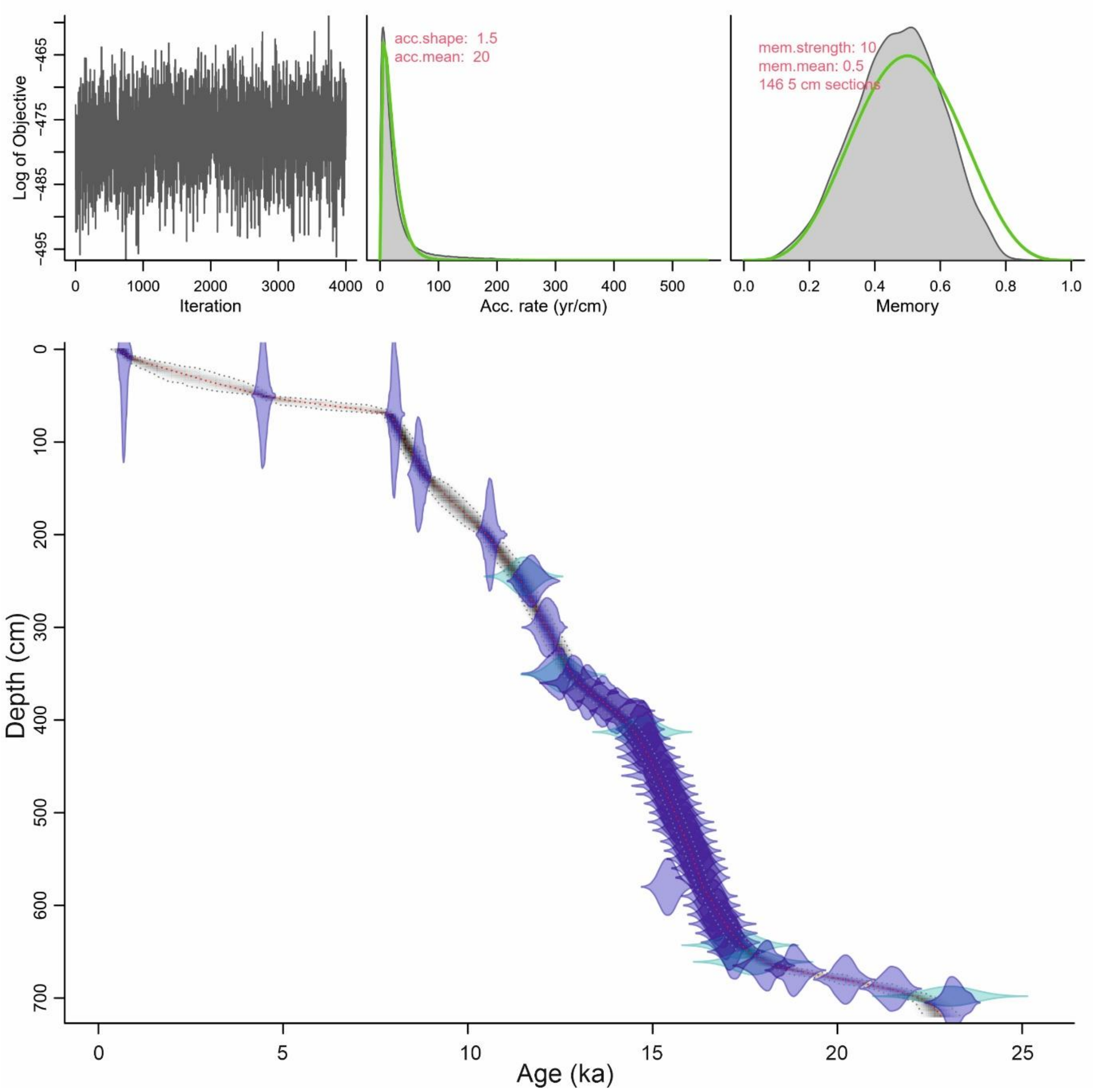

Supplementary Fig. 4: **The age-depth model of marine sediment core GeoB16206-1.** The model is produced using both stratigraphic tie points (aqua symbols) and radiocarbon ages of planktic foraminifera (blue symbols). The R package RBacon[13] was used to build the age-depth model.

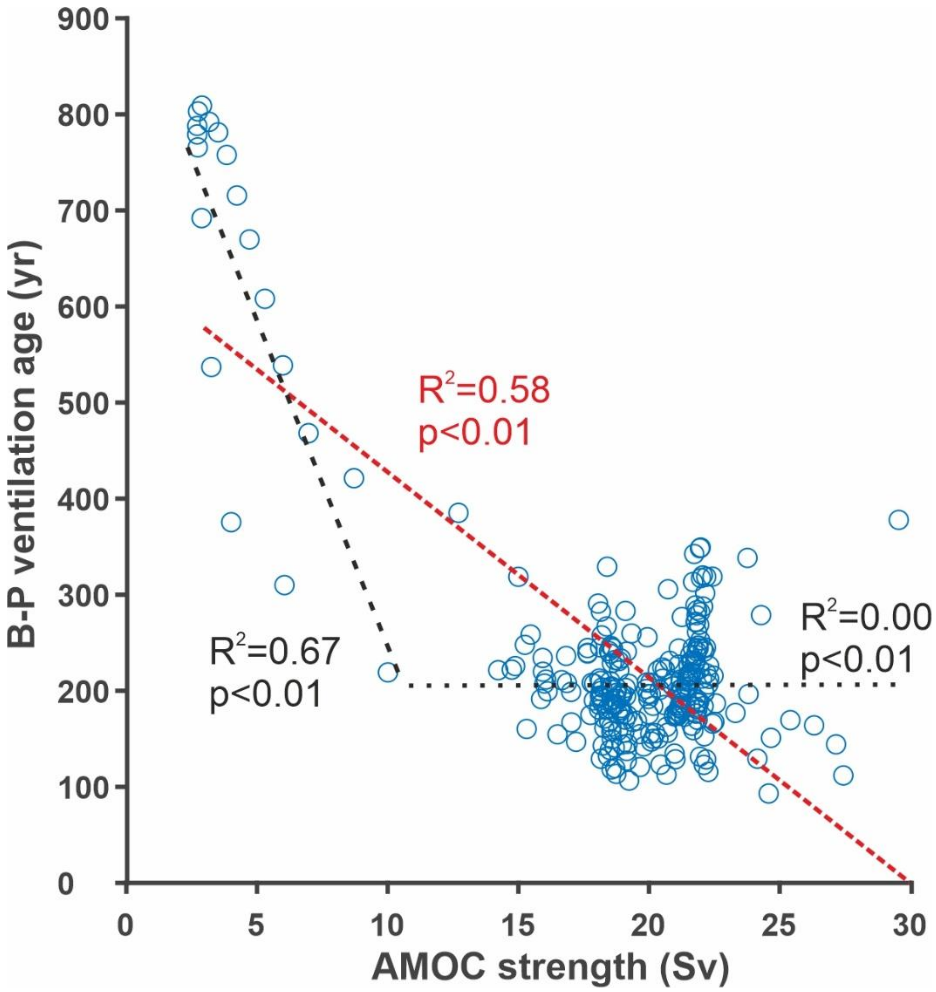

Supplementary Fig. 5: **Correlation between benthic-planktic (B-P) radiocarbon ventilation ages and Atlantic Meridional Overturning Circulation (AMOC) strength based on the CLIMBER-X Earth system model of intermediate complexity[14].** The B-P ventilation ages show a strong negative correlation with AMOC strength, with an R^2 value of 0.58 and a p-value < 0.01. It also appears that the AMOC strength and B-P ventilation age at our core site are strongly linked (R^2=0.67; p-value < 0.01) when AMOC is weak (<10 Sv), while the correlation is weak (R^2=0; p-value < 0.01) during a stronger AMOC (>10 Sv). The absence of a strong relationship during periods of strong AMOC likely results from (i) variability in planktic (P) values that is independent of AMOC strength, and (ii) low benthic (B; thus B-P) values caused by the site's proximity to the North Atlantic (resulting in high relative uncertainties).

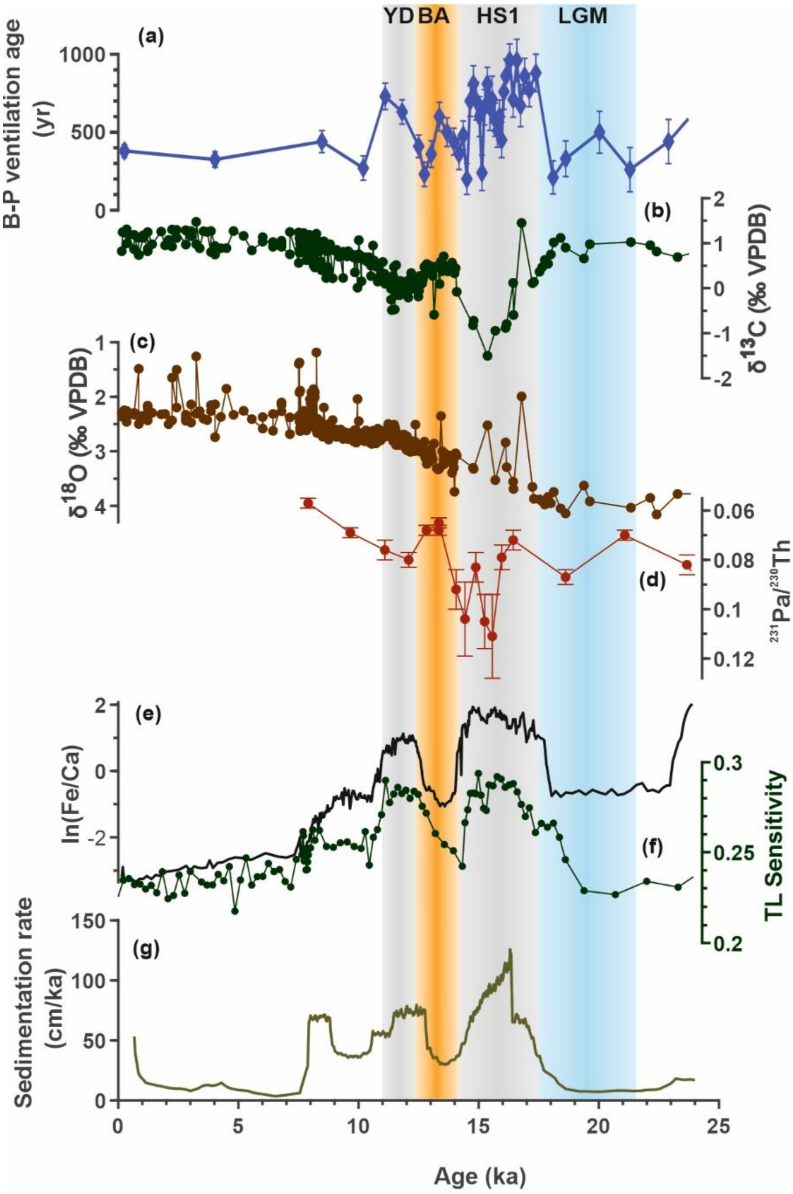

Supplementary Fig. 6: **Geochemical and sedimentological records from marine sediment core GeoB16206-1.** (a) Benthic-planktic (B-P) radiocarbon ventilation age estimates (this study), (b) stable carbon isotopic composition ($\delta^{13}C$) of benthic foraminifera[15], (c) stable oxygen isotopic composition ($\delta^{18}O$) of benthic foraminifera[15], (d) $^{231}Pa/^{230}Th$ ratio[10], (e) ln(Fe/Ca) from bulk sediment[10,15], (f) thermoluminescence (TL) sensitivity[16], and (g) sedimentation rate (this study). Short-term climatic periods are depicted by the vertical bars. Blue: Last Glacial Maximum (LGM); grey: North Atlantic Stadials, i.e., Heinrich Stadial (HS 1) and the Younger Dryas (YD); orange: North Atlantic Interstadial, i.e., Bølling-Allerød (BA).

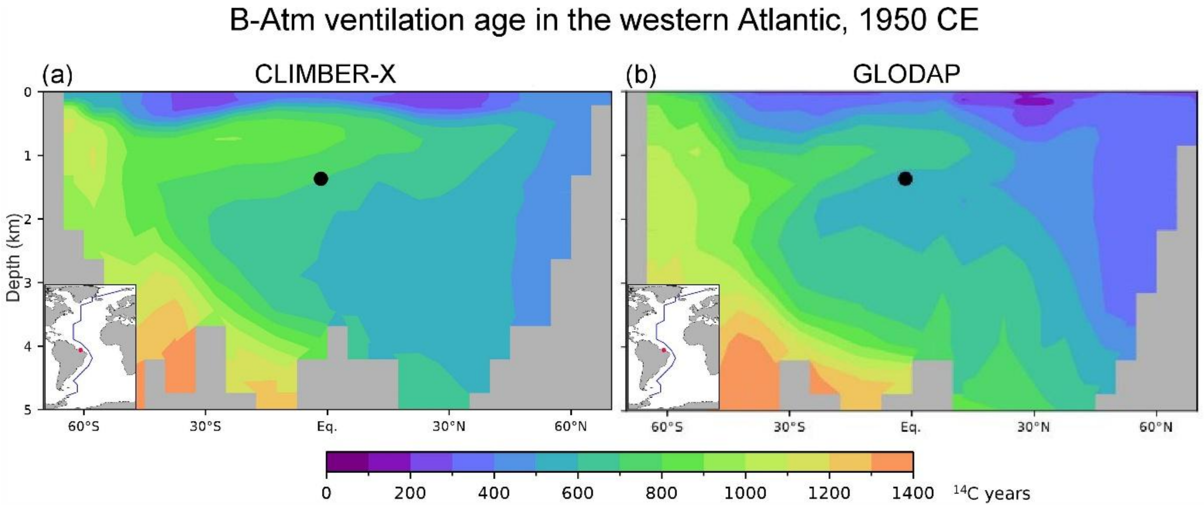

Supplementary Fig. 7: Distribution of B-Atm radiocarbon ages in the western Atlantic in the late Holocene (1950 CE). (a) Simulation results (this study), (b) Reconstruction[17] (shown are gridded data provided by Ref. [18], that were remapped onto the model grid). Filled circles indicate the location of the sediment core GeoB16206-1.

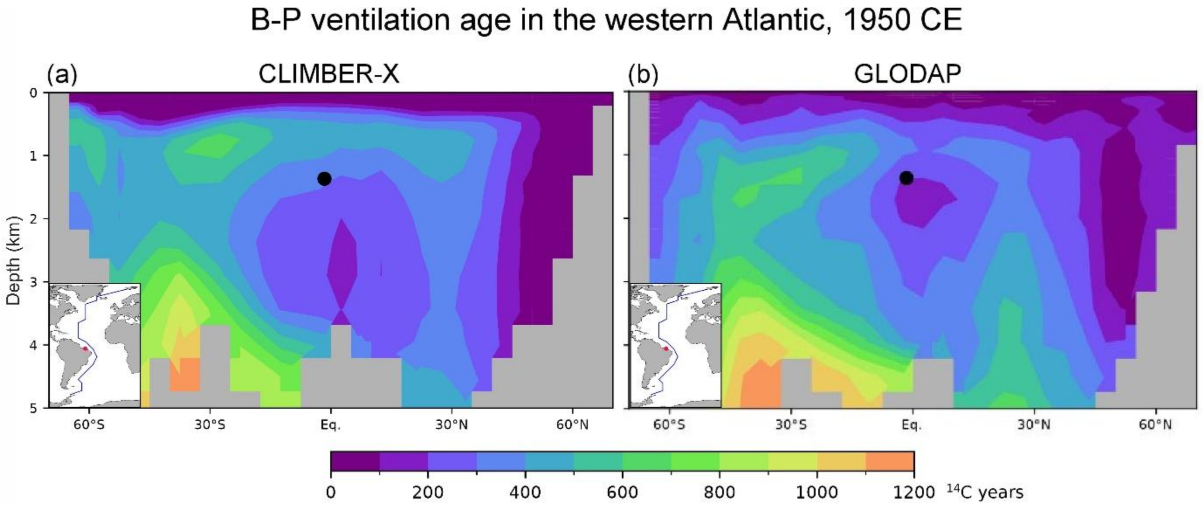

Supplementary Fig. 8: Distribution of B-P radiocarbon ages in the western Atlantic in the late Holocene (1950 CE). (a) Simulation results (this study), (b) Reconstruction[17] (shown are gridded data provided by Ref. [18], that were remapped onto the model grid). Filled circles indicate the location of the sediment core GeoB16206-1. Note that Supplementary Figs. 7 and 8 have different colour scale ranges.

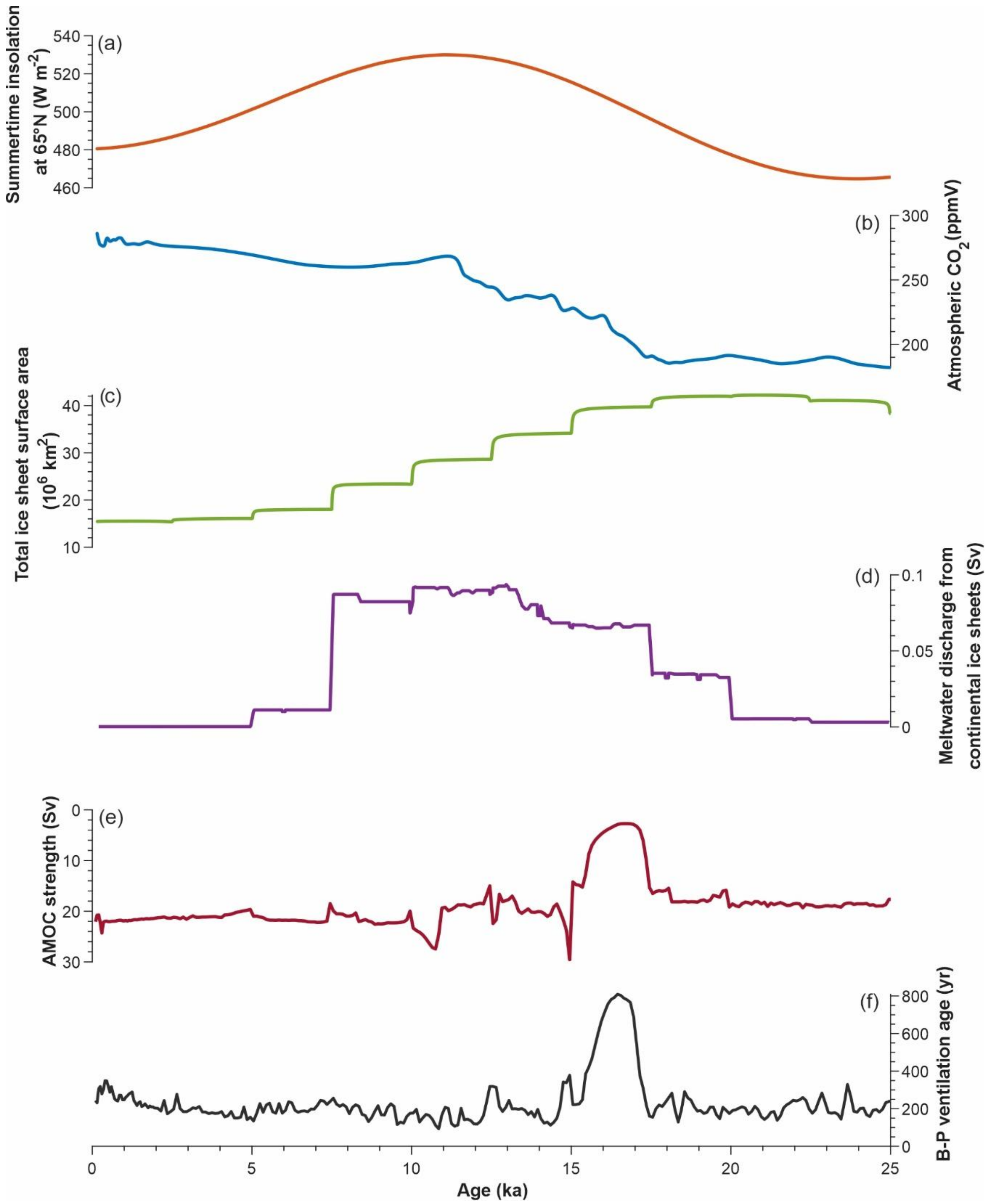

Supplementary Fig. 9: Temporal evolution of model forcings and simulated responses over the last 25 ka. Shown are (a) Summertime insolation at 65ºN[19], (b) Atmospheric CO_2 (Ref. [20]), (c) Total ice-sheet surface area[21], (d) Meltwater discharge from continental ice sheets to the North Atlantic, (e) Atlantic Meridional Overturning Circulation (AMOC) strength, and (f) Benthic-planktic (B-P) ventilation age from the western equatorial Atlantic at 1450 m water depth.

Supplementary Table 1: Chronological tie points for marine sediment core GeoB16206-1 obtained by stratigraphic peak matching as per Supplementary Fig. 2.

Sl. No.	**Core depth (m)**	**Calendar age (ka)**
1	2.5	11.5 ± 0.6
2	3.5	12.6 ± 0.6
3	4.1	14.7 ± 0.7
4	6.4	17.4 ± 0.9
5	6.6	17.7 ± 0.9
6	7.0	23.1 ± 1.2
7	7.4	25.3 ± 1.3
8	7.6	27.8 ± 1.4
9	7.8	28.8 ± 1.4
10	8.0	29.3 ± 1.5

Supplementary Note 1

Radiocarbon analyses on both surface-dwelling planktic (*Globigerinoides ruber and Globigerinoides sacculifer*) and benthic (mixed epifaunal species, excluding agglutinated specimens) foraminifera were performed in this study. Roughly 10 ml of wet sediment samples were collected for processing. The samples were freeze-dried and washed in a 125 µm sieve. The samples were dried and then sieved with a 250 µm sieve. Foraminifera specimens were preferentially picked from >250 µm size fraction. However, in the absence of enough specimens, the 125-250 µm size fraction was also considered. At least 7 mg of planktic and benthic (separately) foraminifera specimens were hand-picked for ^{14}C measurements. A total of 43 samples were analysed for planktic and benthic foraminifera, totalling 86 radiocarbon analyses, out of which 12 planktic ages were reported earlier[10].

Supplementary Note 2

Here, we discuss the possibility that the radiocarbon ventilation age record from sediment core GeoB16206-1 is controlled by processes other than Atlantic Meridional Overturning Circulation (AMOC) strength. The processes discussed below are: (i) the mixing of water masses with different radiocarbon signals; (ii) the effects of bioturbation; and (iii) the influence of local terrestrial carbon. We focus our discussion on Heinrich Stadial 1 (HS1), a period with extremely high ventilation ages and the primary focus of our study. Our radiocarbon ventilation age record shows an abrupt increase during the LGM-HS1 boundary, followed by overall elevated ventilation age values within HS1 (average of 695 yr) (Fig. 2a). Given that a comparable trend (albeit with higher values) has been observed in a nearby sediment core from deeper depths[3], we conclude that the abrupt increase is not abnormal; instead, it appears to be a characteristic feature of mid-depths in the western equatorial Atlantic. Notably similar B-P ventilation ages obtained from the numerical model simulation and our sediment record (Figs. 2a, 2b, 3) further suggest that such values during HS1 are expected.

The sediment core under investigation was collected at a water depth of 1367 m (Section 3). Considering the boundary between Antarctic Intermediate Water (AAIW) and North Atlantic Deep Water (NADW) in this region lies at ~1200 m[22], we carefully examine the effect of AAIW on our radiocarbon signal during HS1. In our western equatorial Atlantic record, HS1 is characterised by a mean B-P ventilation age value of 695 yr (~1367 m water depth). B-P ventilation ages from another core collected at 1000 m water depth (a depth which is effectively bathed by AAIW) from the western equatorial Atlantic[3] show B-P ages (~450 yr) much lower than our site. Hence, a putative larger influence of AAIW during HS1 at our site cannot explain the abruptly higher ventilation ages observed in our record. Changes within northern-sourced waters provide a more reasonable explanation for the very large B-P ventilation ages of core GeoB16206-1. Studies based on authigenic Nd isotopes also suggest no major increase in AAIW contribution during the last deglaciation at depths similar to the core GeoB16206-1[23]. Therefore, we conclude that while there is a possibility of some AAIW mixing, its contribution appears minimal, and the ventilation signal is predominantly driven by NADW during HS1.

Though bioturbation may also alter the foraminiferal radiocarbon signal[24,25], we observe very high sedimentation rates at our site, reaching as much as 100 cm/ka during HS1 (Supplementary Fig. 6g). This suggests an effective preservation of sedimentary sequences and minimal alteration by bioturbation. Thus, we deem it very unlikely that bioturbation substantially altered radiocarbon ventilation ages at our core site.

Degradation of organic matter derived from terrestrial sources may also affect the radiocarbon concentration of the oceanic dissolved inorganic carbon pool. A study[26], based on a sediment core collected midway between the mouths of the Amazon and Parnaíba Rivers (western equatorial Atlantic), showed extremely old organic carbon ages (~2000 yr) during the last glacial-interglacial transition. Interestingly, the authors observed LGM organic carbon ages that are three times older than those of HS1. This is in contrast with our data that show older B-P ventilation ages during HS1 and lower values during the LGM (Figs. 2a, 3). Our study site is influenced by the Parnaíba River and not by the Amazon River. Considering the significantly lower amount of terrestrial sediment input of the Parnaíba River in comparison to the Amazon River[27], we expect a very small influence of terrestrial organic matter at our site. Thus, we confidently reject any effect of local terrestrial carbon influencing radiocarbon ventilation ages at our core site.

Supplementary references

1. Lauvset, S. K. *et al.* GLODAPv2.2022: the latest version of the global interior ocean biogeochemical data product. *Earth Syst. Sci. Data* **14**, 5543–5572 (2022).

2. Stramma, L. & England, M. On the water masses and mean circulation of the South Atlantic Ocean. *J. Geophys. Res. Ocean.* **104**, 20863–20883 (1999).

3. Skinner, L. C. *et al.* Atlantic Ocean Ventilation Changes Across the Last Deglaciation and Their Carbon Cycle Implications. *Paleoceanogr. Paleoclimatology* **36**, 1–21 (2021).

4. Skinner, L. C., Fallon, S., Waelbroeck, C., Michel, E. & Barker, S. Ventilation of the deep southern ocean and deglacial CO_2 rise. *Science.* **328**, 1147–1151 (2010).

5. McManus, J. F., Francois, R., Gherardi, J. M., Keigwin, L. D. & Brown-Leger, S. Collapse and rapid resumption of Atlantic meridional circulation linked to deglacial climate changes. *Nature* **428**, 834–837 (2004).

6. Anderson, R. F. *et al.* Wind-Driven Upwelling in the Southern Ocean and the Deglacial Rise in Atmospheric CO_2. *Science.* **323**, 1443–1448 (2009).

7. Schlitzer, R. Ocean Data View. *Odv.Awi.De* (https://odv.awi.de/, 2023).

8. Ruth, U., Wagenbach, D., Steffensen, J. P. & Bigler, M. Continuous record of microparticle concentration and size distribution in the central Greenland NGRIP ice core during the last glacial period. *J. Geophys. Res. Atmos.* **108**, 4098 (2003).

9. Svensson, A. *et al.* A 60,000 year Greenland stratigraphic ice core chronology. *Clim. Past* **4**, 47–57 (2008).

10. Zhang, Y. *et al.* Origin of increased terrigenous supply to the NE South American continental margin during Heinrich Stadial 1 and the Younger Dryas. *Earth Planet. Sci. Lett.* **432**, 493–500 (2015).

11. Heaton, T. J. *et al.* Marine20 - The Marine Radiocarbon Age Calibration Curve (0-55,000 cal BP). *Radiocarbon* **62**, 779–820 (2020).

12. Willeit, M., Ganopolski, A., Robinson, A. & Edwards, N. R. The Earth system model CLIMBER-X v1.0-Part 1: Climate model description and validation. *Geosci. Model Dev.* **15**, 5905–5948 (2022).

13. Blaauw, M. & Christen, J. A. Flexible paleoclimate age-depth models using an autoregressive gamma process. *Bayesian Anal.* **6**, 457–474 (2011).

14. Masoum, A., Nerger, L., Willeit, M., Ganopolski, A. & Lohmann, G. Paleoclimate data assimilation with CLIMBER-X: An ensemble Kalman filter for the last deglaciation. *PLoS One* **19**, e0300138 (2024).

15. Voigt, I. *et al.* Variability in mid-depth ventilation of the western Atlantic Ocean during the last deglaciation. *Paleoceanography* **32**, 948–965 (2017).

16. Mendes, V. R. *et al.* Thermoluminescence and Optically Stimulated Luminescence Measured in Marine Sediments Indicate Precipitation Changes Over Northeastern Brazil. *Paleoceanogr. Paleoclimatology* **34**, 1476–1486 (2019).

17. Key, R. M. *et al.* A global ocean carbon climatology: Results from Global Data Analysis Project (GLODAP). *Global Biogeochem. Cycles* **18**, 1–23 (2004).

18. Orr, J. C. *et al.* Biogeochemical protocols and diagnostics for the CMIP6 Ocean Model Intercomparison Project (OMIP). *Geosci. Model Dev.* **10**, 2169–2199 (2017).

19. Laskar, J. *et al.* A long-term numerical solution for the insolation quantities of the Earth. *Astron. Astrophys.* **428**, 261–285 (2004).

20. Köhler, P., Nehrbass-Ahles, C., Schmitt, J., Stocker, T. F. & Fischer, H. A 156 kyr smoothed history of the atmospheric greenhouse gases CO_2, CH_4, and N_2O and their radiative forcing. *Earth Syst. Sci. Data* **9**, 363–387 (2017).

21. Gowan, E. J. *et al.* A new global ice sheet reconstruction for the past 80,000 years. *Nat. Commun. 2021 121* **12**, 1–9 (2021).

22. Talley, L. D. Closure of the global overturning circulation through the Indian, Pacific, and southern oceans. *Oceanography* **26**, 80–97 (2013).

23. Lippold, J. *et al.* Deep water provenance and dynamics of the (de)glacial Atlantic meridional overturning circulation. *Earth Planet. Sci. Lett.* **445**, 68–78 (2016).

24. Stott, L. D. How old is too old? Implications of averaging ^{14}C-Based estimates of ventilation age to assess the Pacific Ocean's role in sequestering CO_2 in the past. *Quat. Sci. Rev.* **310**, 108122 (2023).

25. Broecker, W., Mix, A., Andree, M. & Oeschger, H. Radiocarbon measurements on coexisting benthic and planktic foraminifera shells: potential for reconstructing ocean ventilation times over the past 20,000 years. *Nucl. Instruments Methods Phys. Res. Sect. B Beam Interact. with Mater. Atoms* **5**, 331–339 (1984).

26. Nace, T. E. *et al.* The role of North Brazil Current transport in the paleoclimate of the Brazilian Nordeste margin and paleoceanography of the western tropical Atlantic during the late Quaternary. *Palaeogeogr. Palaeoclimatol. Palaeoecol.* **415**, 3–13 (2014).

27. Furquim, J. E., Lima, W. & Medrado Da Silva, E. Suspended sediment fluxes in the large river basins of Brazil. (2005).